Stepwise Iodide-Free Methanol Carbonylation via

Methyl Acetate Activation by Pincer Iridium

Complexes

Changho Yoo^{1,2} and Alexander J. M. Miller^{1,*}

¹ Department of Chemistry, University of North Carolina at Chapel Hill, Chapel Hill, NC 27599-

3290, United States.

² Green Carbon Research Center, Korea Research Institute of Chemical Technology (KRICT),

Daejeon 34114, Republic of Korea

E-mail: ajmm@email.unc.edu

ABSTRACT. Iodide is an essential promoter in the industrial production of acetic acid via

methanol carbonylation, but it also contributes to reactor corrosion and catalyst deactivation. Here

we report that iridium pincer complexes mediate the individual steps of methanol carbonylation to

methyl acetate, in the absence of methyl iodide or iodide salts. Iodide-free methylation is achieved

under mild conditions by an aminophenylphosphinite pincer iridium(I) dinitrogen complex

through net C–O oxidative addition of methyl acetate to produce an isolable methyliridium(III)

acetate complex. Experimental and computational studies provide evidence for methylation via

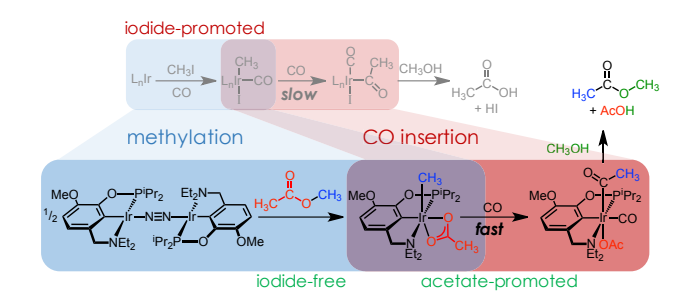
initial C-H bond activation followed by acetate migration, facilitated by amine hemilability.

Subsequent CO insertion and reductive elimination in methanol solution produced methyl acetate

1

and acetic acid. The net reaction is methanol carbonylation to acetic acid using methyl acetate as a promoter, alongside conversion of an iridium dinitrogen complex to an iridium carbonyl complex. Kinetic studies of migratory insertion and reductive elimination reveal essential roles of the solvent methanol and distinct features of acetate and iodide anions that are relevant to the design of future catalysts for iodide-free carbonylation.

Table of Contents Graphic.



Keywords: Carbonylation, C-O activation, Methyl acetate, Iridium, Pincer ligand

Introduction

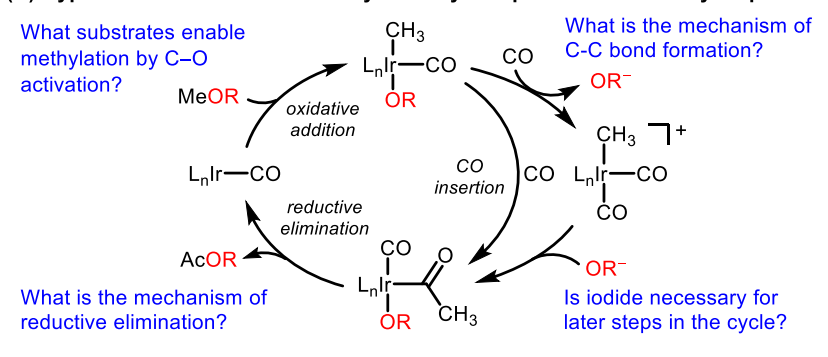
The production of acetic acid by methanol carbonylation is currently one of the largest scale industrial processes based on homogeneous catalysis, with annual capacity exceeding 13 million tons.^{1,2} Iodide salts or methyl iodide are essential promoters in the catalytic reaction. Hydroiodic acid and methyl iodide are continually generated *in situ* during the process, with the latter initiating the organometallic catalytic cycle by forming a metal methyl species (Scheme 1).^{3–5} However, the need for iodide has serious disadvantages. Methyl iodide and hydroiodic acid are toxic and corrosive, necessitating expensive safety and engineering controls.^{4,6} Iodide also complicates the chemical pathways. In the rhodium-catalyzed ("Monsanto") process, the

precipitation of RhI₃ is a significant catalyst deactivation pathway. ⁴⁻⁶ In the iridium-catalyzed ("Cativa") process, iodide inhibits CO migratory insertion by generating inactive iodide-bound species, necessitating the use of halide abstractors such as ruthenium(II) salts to achieve high activity. ⁴⁻⁷ Therefore, development of low-iodide or iodide-free processes has attracted the attention of both academic and industrial scientists. Advances in iodide-free carbonylation have been driven by heterogeneous Lewis acid catalysts. ⁸⁻¹⁶ While promising, these systems typically require temperatures of ca. 200 °C and produce dimethyl ether as an undesired byproduct. Homogeneous molecular catalysts for methanol carbonylation without iodide promoters remain elusive.

Scheme 1. Comparison of a carbonylation process using iodide and a possible iodide-free process via C–O activation.

(B) Hypothetical iodide-free carbonylation cycle: questions about key steps

iodide-promoted cycle



The primary challenge in halide-free carbonylation with molecular catalysts is accessing the organometallic methyl complexes that mediate C–C bond formation. Most catalysts must rely on potent alkylating agents such as methyl iodide to form the M–CH₃ unit (Scheme 1A). One strategy to minimize methyl iodide concentrations utilizes quaternary ammonium iodide or phosphonium iodide salts that produce only equilibrium amounts of methyl iodide under the reaction conditions of carbonylation.¹⁷ Iodide is still required, however, and many of the concerns noted above remain in these systems.

An alternative approach involves designing organometallic catalysts capable of C–O oxidative addition (Scheme 1B), avoiding the need for H₃C–I oxidative addition altogether. The most obvious and ideal reactant would be CH₃OH, but we are not aware of any well-defined C–O oxidative addition reactions of methanol. We hypothesized that methyl acetate (MeOAc) could be a more promising candidate than methanol for halide-free alkylation, because acetate is a better leaving group than hydroxide. Methyl acetate is also a coproduct and common solvent for methanol carbonylation.^{1–4} However, examples of methyl acetate C_{sp3}–O bond cleavage are extremely limited and generally produce product mixtures.^{18–21} In an encouraging example, the Goldman group showed that initial C–H bond activation at an iridium center initiates net C_{sp3}–O oxidative addition of methyl acetate.²¹ However, the reaction required prolonged heating at 125 °C and suffered from unwanted C–H activation of *tert*-butyl substituents of the tertiary phosphine donor, precluding isolation of the methyliridium acetate product.

Our group previously reported catalytic methanol carbonylation using aminophenylphosphinite (NCOP) pincer iridium complexes in the presence of methyl iodide and metal salt promoters.²² Although partial dissociation of the ligand was observed under catalytic conditions, stoichiometric studies established the viability of each reaction step, including Lewis

acid promotion of the C–C bond-forming migratory insertion step.²³ We recently isolated a NCOP iridium(I) dinitrogen compound and found that it facilitates decarbonylative C–O bond cleavage of ethers, initiated by C–H bond activation.²⁴ These results led us to a stepwise study on iodide-free methanol carbonylation using methyl acetate as the methylating reagent. Here, the aminophenylphosphinite ligand supports clean formal oxidative addition of methyl acetate to generate an isolable methyliridium acetate complex for the first time. The subsequent migratory insertion and reductive elimination steps could then be studied individually, enabling a detailed understanding of how iodide-free conditions with acetate ions compare to conditions with iodide ions (helping to address the questions in Scheme 1B). The elimination process, in particular, has previously eluded careful interrogation in iridium-catalyzed carbonylation, leading to conflicting views on whether C–O or C–I bond formation occurs from the acetyl intermediate in the Cativa process.^{3,25–27} The present study provides a rare opportunity to directly compare acetyl complex reactivity by either methanolysis to generate methyl acetate directly, or reductive elimination with iodide to generate acetyl iodide as an intermediate.

Result and Discussion

MeOAc activation. Initial studies investigating the activation of MeOAc by previously reported (NCOP)Ir(CO) complexes did not show promising reactivity, despite the ability of these carbonyl complexes to carry out the individual steps and overall catalytic reaction of methanol carbonylation in the presence of methyl iodide.^{22,23} Inspired by the Goldman group's reports of net C–O bond activation via initial C–H bond activation,^{21,28–30} and our own recent observation of ether decarbonylation via C–H bond activation,²⁴ we turned to the dinitrogen complex [($^{MeO-Et}NCOP$)Ir]₂(μ-N₂) (1).

A red solution of **1** and 1 equiv MeOAc in benzene became colorless after heating at 80 °C for 1 h. NMR spectroscopy revealed 75% yield of a new species with a $^{31}P\{^{1}H\}$ NMR signal (δ 133.13) upfield shifted from that of **1** (δ 163.68). A diagnostic upfield methyl resonance in the $^{13}C\{^{1}H\}$ NMR spectrum (δ –29.49, d, J_{PC} = 7.0 Hz) supports the formation of the iridium methyl acetate complex ($^{MeO-Et}NCOP$)Ir(CH₃)(OAc) (**2**) (Figure 1A). Compound **2** was isolated in 42% yield after crystallization from diethyl ether at –35 °C. An X-ray diffraction (XRD) study revealed a pseudo-octahedral coordination with the methyl group *cis* to the pincer phenyl ligand and the acetate ligand in a bidentate (κ^{2}) binding mode (Figure 1B).

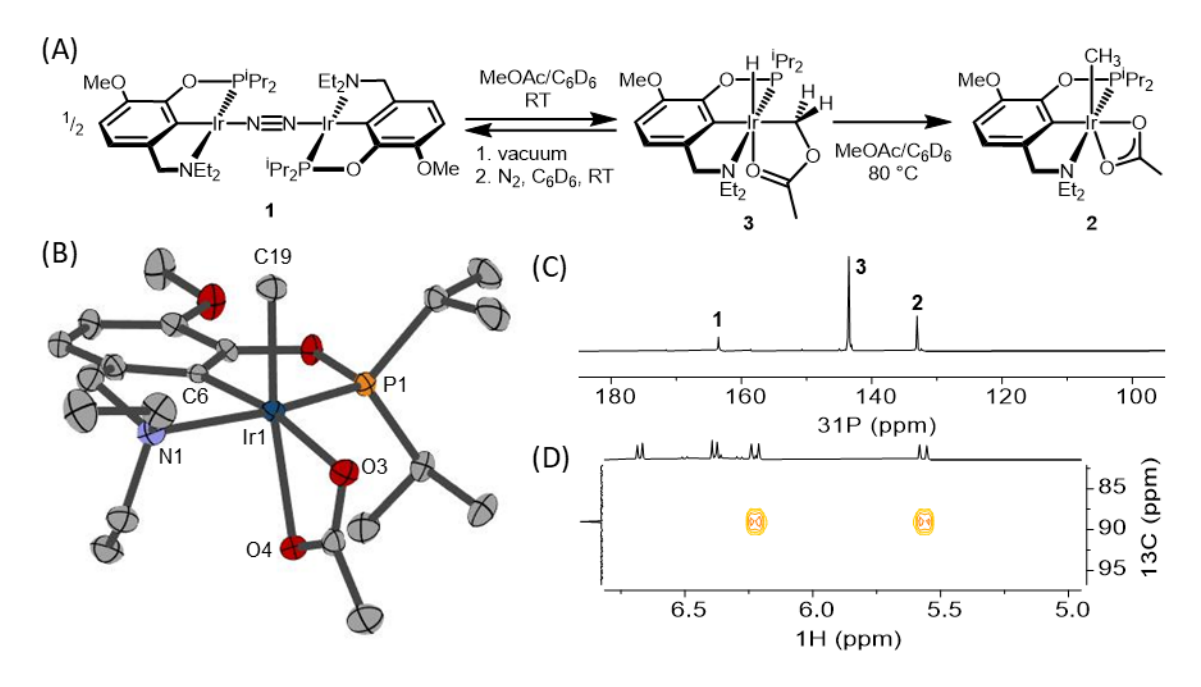


Figure 1. (A) MeOAc activation by **1** via C-H activation. (B) Structural representation of **2**. (C) ³¹P{¹H} NMR spectrum after reaction of **1** and MeOAc at room temperature for 24 hr (D) Partial ¹H-¹³C HSQC spectrum of **3** showing correlation of geminal protons with the carbon in acetoxymethyl (–CH₂OAc) group.

Monitoring the conversion of 1 to 2 by NMR spectroscopy at room temperature revealed an intermediate. In C_6D_6 , the reaction of 1 with 1 equiv MeOAc was slow (~60% conversion of 1 in 10 h at room temperature) and resulted in multiple species along with trace amounts of 2. When

the reaction was instead conducted in 1:1 mixture of MeOAc: C_6D_6 (approximately 110 equiv MeOAc relative to 1) at room temperature, however, a prominent new ^{31}P resonance grew in at δ 143.52 (Figure 1C). The intermediate 3 features a hydride resonance at δ –26.11 (d, J_{PH} = 28.6 Hz) in the ^{1}H NMR spectrum, indicating a weak donor *trans* to the hydride. ^{1}H - ^{13}C HSQC and HMBC NMR experiments enabled assignment as ($^{MeO-Et}NCOP$)Ir(H)(κ^2C , O-CH $_2OAc$) (3, Figure 1A, and Figures S4-S8). The CH $_2OAc$ group was identified by the two diastereotopic geminal protons at δ 6.23 and δ 5.57 (d, $^{1}J_{HH}$ = 11.3 Hz) and ^{13}C resonance at δ 89.49 (Figure 1D). After 24 h at room temperature, a mixture of 1 (10%), 3 (70%) and 2 (20%) was obtained (Figure 1C). Heating this reaction mixture at 80 $^{\circ}C$ for 1 h resulted in complete consumption of 1 and 3 to produce 2 in 75% yield. If instead of heating, a similarly obtained mixture containing 1, 2, and 3 was exposed to vacuum to remove the MeOAc, only 1 and 2 remained after the solids were redissolved in C_6D_6 under N_2 . The formation of 3 from 1 is therefore a reversible process, while the formation of 2 is not.

The net C–O oxidative addition of methyl acetate mediated by the (MeO-EtNCOP)Ir center is noteworthy for proceeding in high yield under relatively mild conditions. For comparison, MeOAc activation by a diphosphine-based iridium pincer complex utilized by Goldman *et al.* required heating at 125 °C due to formation of a stable intermediate in which methylene inserts into the iridium–aryl bond of the pincer backbone.²¹ Under the reaction conditions required to finally reach the methyliridium acetate complex, there is a competing side reaction involving C–H bond activation of a *tert*-butyl phosphine substituent, preventing isolation of (IBu4PCP)Ir(Me)(OAc) (IBu4PCP is 2,6-(IBu2PCH2)2-C₆H₃). In contrast, the present complex 2 is generated even at room temperature, is produced in high yield at 80 °C according to NMR spectroscopy, and can be isolated in a thermally-stable crystalline form.

To understand why the aminophenylphosphinite pincer ligand supports cleaner reactivity under milder conditions, the detailed mechanism of net C–O oxidative addition was examined using density functional theory (DFT). Four pathways were considered: direct C–O oxidative addition, and three pathways that start with C–H bond activation (Figure 2). The experimental observation of alkyl hydride intermediate **3** provides strong evidence against a direct C–O oxidative addition pathway, instead supporting initial oxidative addition of a C–H bond of MeOAc (Figure 1A). Accordingly, the barrier to C–H activation was computed to be ca. 30 kcal/mol while the barrier to direct C–O oxidative addition was computed to be 52.1 kcal/mol.

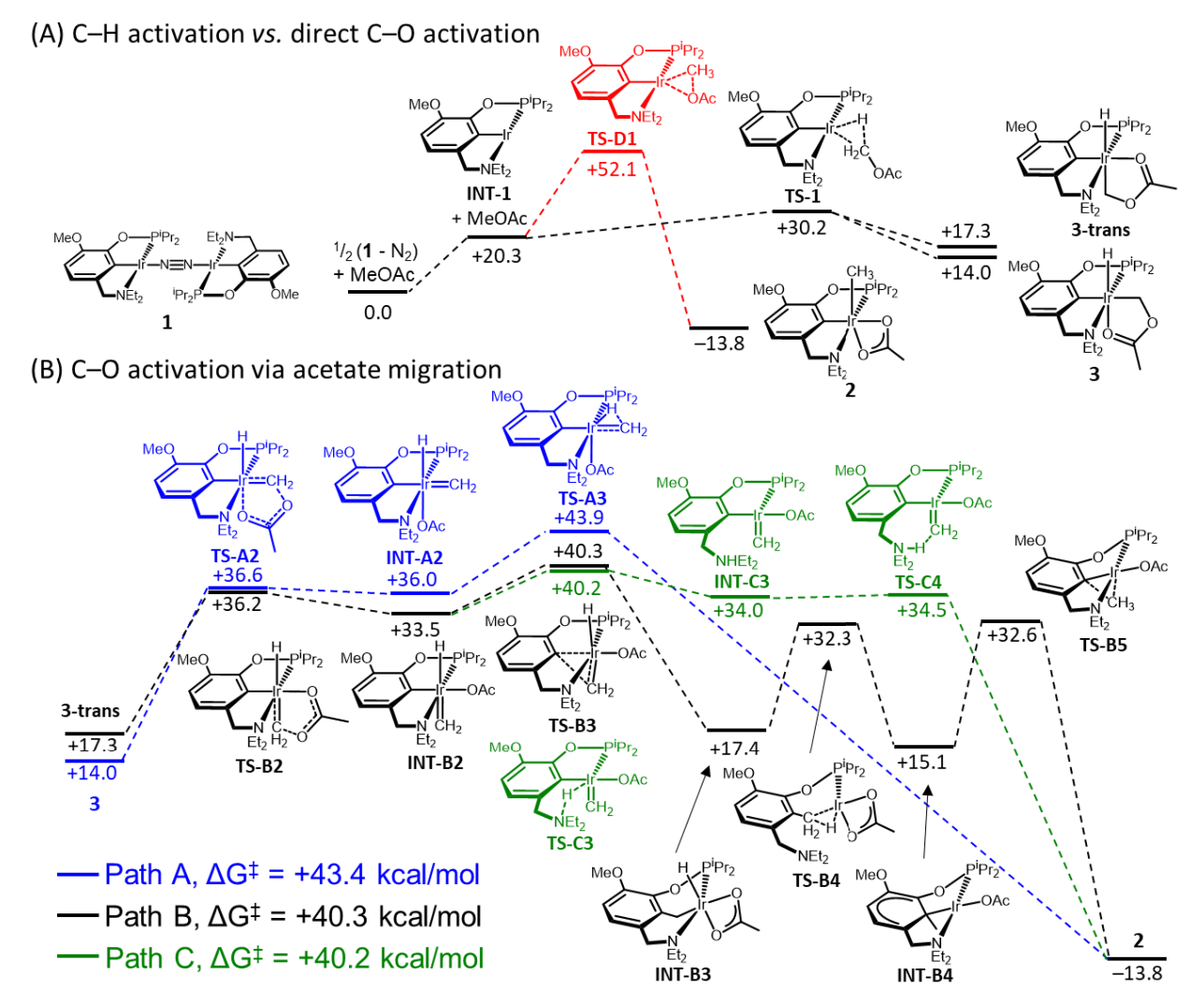


Figure 2. Calculated Gibbs free energies (kcal/mol) for reaction of 1 with MeOAc via C–H activation (black and blue) and direct C–O activation (red). Values of G are given relative to ½ (1

 $-N_2$) + MeOAc. The free energies correspond to a reference state of 1 M concentration for each species participating in the reaction and T = 298.15 K.

Possible C–H activation routes were evaluated in detail through DFT calculations (Figure 2). Paths A, B and C all start with N₂ dissociation and C–H activation by the coordinatively unsaturated intermediate **INT-1**. The resulting hydride species **3** is higher in energy than **1** ($\Delta G = +14.0 \text{ kcal/mol}$) due to unfavorable N₂ dissociation ($\Delta G = +20.3 \text{ kcal/mol}$). However, in experimental practice the reaction may be driven by low N₂ solubility at the elevated temperature and/or the excess amount of MeOAc, consistent with our experimental observation of equilibrium formation of **3** with ~110 equiv of MeOAc at room temperature.

In Path A, alkyl hydride **3** undergoes acetate migration to produce an intermediate with a methylidene ligand *cis* to the hydride (**INT-A2**), likely by retro-electrocyclization (**TS-A2**, ΔG^{\ddagger} = +36.2 kcal/mol). The methyl species **2** can be generated by 1,1-hydride migration (**TS-A3**, ΔG^{\ddagger} = +43.9 kcal/mol), which has highest activation barrier in overall reaction.

In Path B, C–H bond activation produces **3-trans**, in which the acetoxymethyl carbon ($-CH_2OAc$) is *trans* to hydride ($\Delta G = +3.3$ kcal/mol relative to **3**). Both **3-trans** and **3** are accessed by the same early C–H activation transition state **TS-1**, with barrierless coordination of oxygen either *cis* or *trans* to the hydride producing the respective isomers of **3** (Figure S46 and S47). Complex **3-trans** could also form by isomerization of **3**, either via **TS-1** ($\Delta G = +16.2$ kcal/mol relative to **3**) or via oxygen dissociation, bending of the Ir–CH₂OAc bond, and recoordination of oxygen ($\Delta G < 14$ kcal/mol based on the potential energy surface scan, Figure S48). The subsequently formed *trans*-methylidene (**INT-B2**) cannot undergo direct C–H reductive elimination with hydride, so it is first inserted into the Ir–C_{aryl} bond to give **INT-B3**. This process has the highest energy TS in Path B (**TS-B3**, $\Delta G^{\ddagger} = +40.3$ kcal/mol). The subsequent C–H

reductive elimination yields **INT-B4**, in which the methyl from methyl acetate is added on the aromatic backbone of the NCOP ligand. In the transition state (**TS-B4**), the amine donor is dissociated, enabling a geometric distortion that facilitates concerted reductive elimination between adjacent hydride and ArCH₂ ligands. Finally, the C–C oxidative addition of the Ar–CH₃ bond in **INT-B4** produces the methyl species **2**.

In Path C, the amine arm acts as a proton relay. From *trans*-methylidene intermediate **INT-B2**, Ir–N bond cleavage and N–H bond formation occurs (amine deprotonation of the hydride ligand) to give **INT-C3**. The ammonium group then transfers the proton to the methylidene ligand to form the methyl species **2**. The highest activation barrier is deprotonation of hydride by the amine (**TS-C3**, $\Delta G^{\ddagger} = +40.2 \text{ kcal/mol}$).

All pathways involving initial C–H activation (Path A, B and C, Figure 2) are plausible based on the computational data, and have significantly lower computed activation barriers than the direct C–O bond activation (Path D). The slightly lower overall free energy spans for Paths B and C relative to Path A are attributed to hemilability of the amine donor of the pincer ligand. A mechanism akin to Path B was proposed in C–O and C–C bond activation by diphosphine-based pincer rhodium and iridium complexes, ^{21,31–33} however a higher barrier is encountered in the (^{18u4}PCP)Ir analogue to **TS-B4**. ²¹ The lower barrier of **TS-B4** for the (NCOP)Ir system is ascribed to amine hemilability. Whereas no phosphine dissociation was apparent in calculations of the (NCOP)Ir system, thus requiring an isomerization sequence before reductive elimination, the (NCOP)Ir system does not require any geometric isomerization and instead amine dissociation is apparent in **TS-B4** (Figure 2), which would provide increased flexibility for low-barrier C–H reductive elimination. Path C also features a relatively low-barrier pathway enabled by a labile amine donor acting as a hydride-to-methylidene proton shuttle. Hemilability of the amine donor

may therefore be responsible for the relatively low barriers, and thus the clean reactivity of (NCOP)Ir complex under mild conditions compared to the (^{tBu4}PCP)Ir system.

Having identified a clean methylation reaction involving methyl acetate, we individually examined CO migratory insertion and acetyl reductive elimination steps.

CO migratory insertion. Addition of 1 atm CO to a solution of methyliridium acetate complex 2 at room temperature in C₆D₆ immediately produced the carbonyl complex (MeO-EtNCOP)Ir(CH₃)(OAc)(CO) (4-trans, where trans indicates the relative orientation of the carbonyl and methyl ligands). The methyl resonance was found at δ 0.71 in the ¹H NMR spectrum. Heating a solution of 4-trans at 80 °C in C₆D₆ under CO produced a new species with a methyl resonance shifted to δ 0.47. The new species was assigned as the isomer (MeO-EtNCOP)Ir(CH₃)(CO)(OAc) (4-cis, Figure 3A). The ¹³C{¹H} NMR spectrum of 4-cis confirms the presence of a CO ligand (δ 175.75) and a methyl ligand (δ -30.92, d, J_{PC} = 7.2 Hz). The infrared (IR) spectrum of 4-cis is consistent with a single carbonyl ligand ($\nu_{co} = 2023~\text{cm}^{-1}$) and a monodentate acetate ligand ($\nu_{co} = 1622 \text{ cm}^{-1}$, $\nu_{co} = 1316 \text{ cm}^{-1}$). After 36 h heating at 80 °C, the ratio of 4-trans:4-cis was 1:10. Higher purity samples of 4-cis could be obtained from the reaction of (MeO-EtNCOP)Ir(CO) (6) with MeI to produce (MeO-EtNCOP)Ir(CH₃)(CO)(I) (5-cis), followed by iodide abstraction with AgOAc (Figure 3). Heating a solution of pure 4-cis under N₂ in C₆D₆ at 80 °C produced a mixture of 4-trans and 4-cis, with a similar ratio as observed when after heating **4-trans**, confirming that the two isomers are in equilibrium ($\Delta G = -1.6(1)$ kcal/mol favoring formation of 4-cis). DFT calculations also predict that 4-cis is thermodynamically favored over 4trans ($\Delta G = -2.9 \text{ kcal/mol}$ in the gas phase).

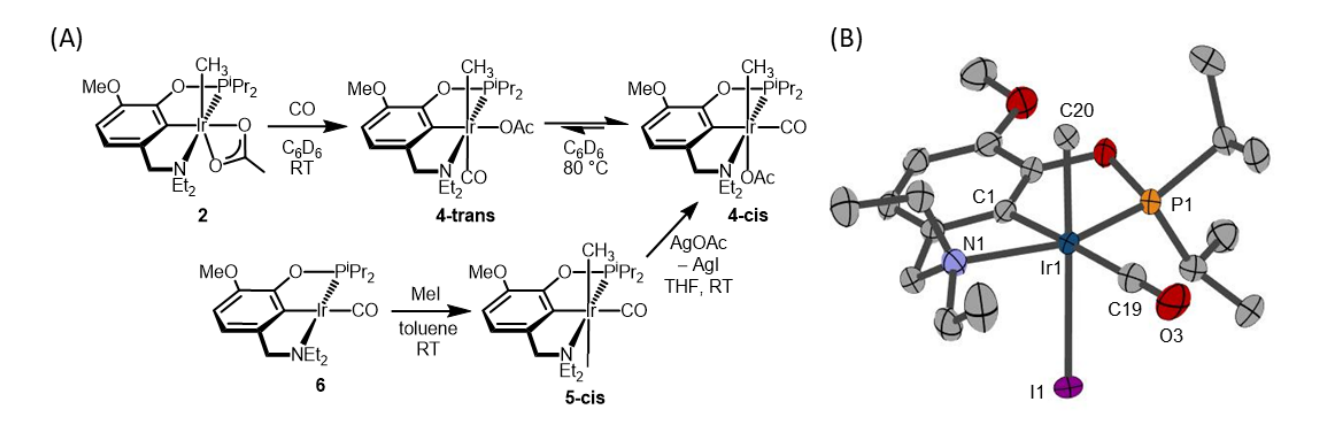


Figure 3. (A) Synthesis of carbonyl species. (B) Structural representation of **5-cis** from X-ray diffraction analysis, with ellipsoids drawn at 50% probability level. Hydrogen atoms are omitted for clarity.

No CO migratory insertion to form an acetyl product was observed during thermolysis of **4-cis** under CO in C₆D₆. Similarly, refluxing solutions of **4-cis** in CD₂Cl₂ or CD₃CN under 1 atm CO overnight resulted in no C–C bond formation. Trace amounts of (MeO-EtNCOP)Ir(CO) (6) were the only new product observed.

Reactions in methanol, however, tell a different story (Scheme 2). Addition of 1 atm CO to a solution of **4-cis** in CD₃OD at ambient temperature resulted in formation of a new methyl species ($^{31}P\{^{1}H\}$ NMR δ 142.93) in approximately 70% yield within 5 hours. New methyl resonances (^{1}H NMR δ 0.60, d, $J_{PH} = 2.0$ Hz and $^{13}C\{^{1}H\}$ NMR δ –9.22, d, $J_{PC} = 6.9$ Hz) were found slightly downfield of those in **4-cis**. Two carbonyl carbon resonances were found at δ 173.17 and 168.75 in the ^{13}C NMR spectrum, indicating that the new product is a methyl dicarbonyl complex with an outer-sphere acetate counter-anion, [($^{MeO-Et}NCOP$)Ir(CH₃)(CO)₂][OAc] ([7][OAc], Scheme 2). Monitoring the reaction over 18-22 hours did not lead significant changes in the ratio of products, suggesting that the reaction achieved equilibrium ($K_{eq} = 24.0(3)$, $\Delta G = -1.88(1)$ kcal/mol).

Heating a solution of [7][OAc] in CD₃OD under 1 atm CO at 65 °C led to complete conversion to the carbonyl complex 6 (84% yield) after 2 days, with concomitant production of partially-deuterated methyl acetate CH₃COOCD₃ (¹H NMR δ 2.02, 106% yield) and acetic acid CH₃COOD (¹H NMR δ 1.92, 42% yield) (Scheme 2A). The partially-deuterated methyl acetate could form upon reductive elimination of acetyl with CD₃OD solvent, or upon reductive elimination of methyl and acetate groups from [7][OAc] (without formation of the acetyl intermediate) followed by transesterification of methyl acetate with CD₃OD solvent (Scheme 2B). In the former case, a total of 2 equiv of acetyl products (CH₃COOCD₃ + CH₃COOD) would be formed, whereas only 1 equiv is expected in the latter case (Scheme 2B). The formation of ~1.5 equiv. of acetyl products indicates acetyl formation via carbonylation. In order to confirm the origin of the acetic acid and methyl acetate products, an isotopic labeling experiment was performed.

Scheme 2. (A) Carbonylation of **4-cis** in CD₃OD. (B) Possible routes for formation of **6** and acetyl products.

$$(A) \qquad \underset{\text{MeO}}{\text{MeO}} \qquad \underset{\text{NEt}_2}{\text{CD}_3\text{OD}} \qquad \underset{\text{NEt}_2}{\text{CO}} \qquad \underset{\text{NEt}_2}{\text{CD}_3\text{OD}} \qquad \underset{\text{NEt}_2}{\text{MeO}} \qquad \underset{\text{NEt}_2}{\text{CD}_3\text{OD}} \qquad \underset{\text{NE}_2}{\text{CD}_3\text{OD}} \qquad \underset{NE}_2}{\text{CD}_3\text{OD}} \qquad \underset{\text{NE}_2}{\text{CD}_3} \qquad \underset{\text{NE}_2}{\text{CD}_3\text{$$

Reaction of 6 with 13 CH₃I, followed by iodide abstraction with AgOAc, afforded the 13 C-labeled methyl complex ($^{MeO-Et}$ NCOP)Ir(13 CH₃)(CO)(OAc) (4-cis- 13 C). After heating a CD₃OD solution of 4-cis- 13 C at 65 °C under 1 atm CO for 18 h, a 13 C-enriched signal was detected at δ 20.48 in the 13 C NMR spectrum, with a corresponding doublet (δ 2.02, 1 J_{CH} = 129.4 Hz) in the 1 H NMR spectrum indicating the formation of labeled methyl acetate 13 CH₃COOCD₃ by carbonylation and elimination of acetyl with CD₃OD (Scheme 3A). The reaction is balanced by proton transfer from methanol to acetate, forming acetic acid without 13 C enrichment, CH₃COOD (1 H NMR δ 1.93, s), as a coproduct. Since 4-cis can be produced from the activation of methyl acetate followed by CO addition, the overall reaction is methanol carbonylation to acetic acid using methyl acetate as a methylating promoter (Scheme 3B).

Scheme 3. Isotopic labelling experiment of 4-cis-¹³CH₃ carbonylation.

(A)
$$\frac{^{13}\text{CH}_3}{^{13}\text{CH}_3}$$
 $\frac{^{13}\text{CH}_3}{^{13}\text{CO}}$ $\frac{^{13}\text{CH}_3}{^{13}\text{CO}}$

Solvent effects on CO insertion: facilitating acetate dissociation. The acceleration of migratory insertion by methanol solvent has been observed with the Cativa catalyst.³⁴ Similarly, the carbonylation of methyl complex **4-cis** was only observed in methanol solution. Given that methanol was the only solvent in which CO substituted the acetate ligand in **4-cis**, we hypothesized that formation of cationic dicarbonyl species [7]⁺ was key for CO migratory insertion. The DFT-calculated transition state energies for CO migratory insertion in **4-cis** and [7]⁺ are compared in Figure 4A. Both transition state structures are consistent with the usual mechanism of methyl

migration to the CO ligand (Figure 4B and 4C). The barrier for neutral acetate species **4-cis** is high $(G_{TS,4-cis} = +48.1 \text{ kcal/mol})$; the migratory insertion barrier for cationic dicarbonyl [7]⁺ is ca. 20 kcal/mol lower $(G_{TS,7+} = +27.8 \text{ kcal/mol})$. The cationic species is expected to possess a more electrophilic CO ligand, facilitating nucleophilic attack by the methyl ligand.^{7,35} In addition, the methyl group in [7]⁺ may be more nucleophilic due to the strong *trans* influence of the carbonyl ligand relative to acetate. Support for this notion comes from comparisons (Table S13) of calculated Ir–CH₃ bond distances in [7]⁺ (2.14 Å) *vs.* **4-cis** (2.11 Å) and comparisons of NBO charges on the methyl carbon in [7]⁺ (-0.80) *vs.* **4-cis** (-0.77). The NBO charge on the carbonyl carbon is similar in magnitude but opposite in sign, consistent with a more electrophilic CO ligand in [7]⁺ compared to **4-cis**.

The calculations suggest methanol solvation does not significantly impact the CO insertion barrier for either **4-cis** or [7]⁺ (Figure 4A). Instead, we propose that the primary role of the methanol solvent is to promote pre-equilibrium acetate dissociation through dipole and hydrogen bonding interactions. The calculations agree that substitution of acetate by CO is more accessible in methanol ($\Delta G_{\rm diss}$ = +6.6 kcal/mol) than in CH₂Cl₂ (+14.6 kcal/mol) (Figure 4A). The experimental data shows that the acetate dissociation and CO binding is slightly exergonic ($\Delta G_{\rm diss}$ = -1.88(1) kcal/mol), which is in reasonable agreement with DFT when considering that the calculations do not account for explicit solvent interactions such as hydrogen bonding interactions between the methanol solvent and acetate anion.

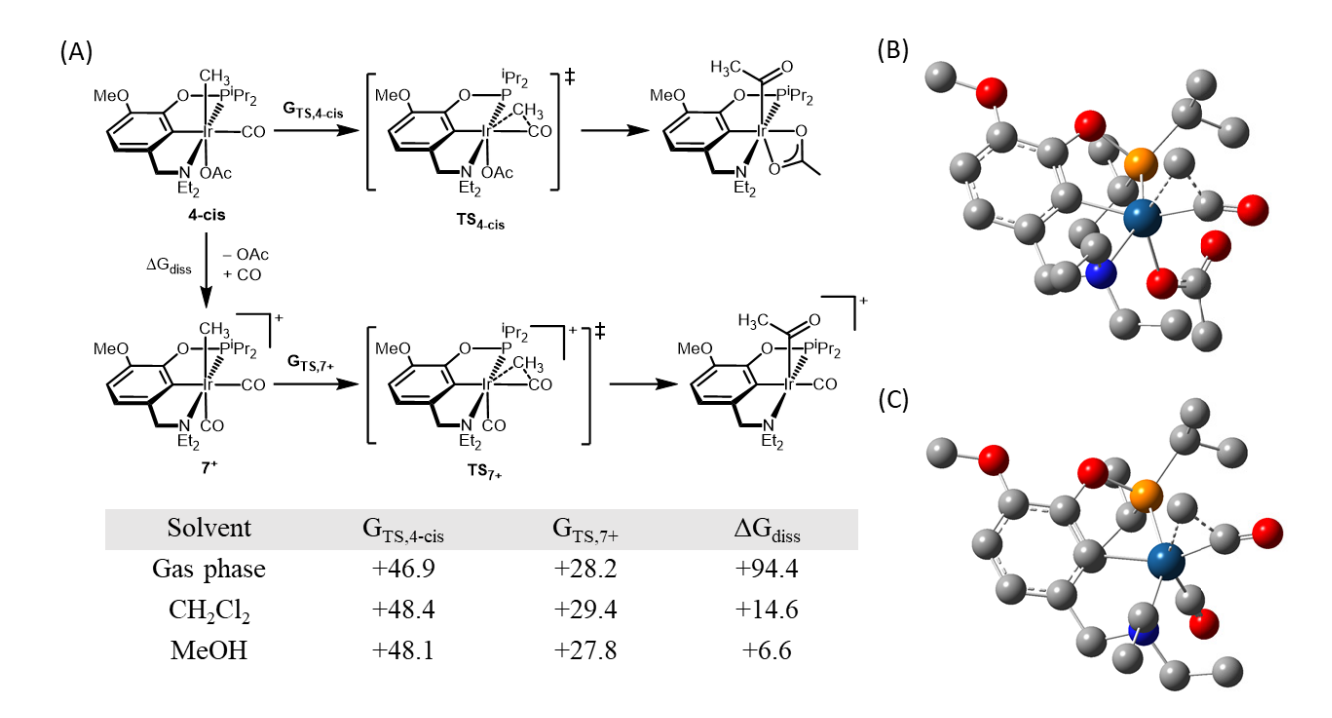


Figure 4. Calculated transition state energy (free energies in kcal/mol) for CO insertion in **4-cis** and [7]⁺, and acetate dissociation energy (A). Calculated transition state structures for migratory insertion in **4-cis** (B) and [7]⁺(C).

The DFT calculations suggests that generation of a cationic species is important for CO migratory insertion. This is consistent with a body of experimental evidence that relatively electron-deficient cationic alkyl carbonyl complexes undergo fast migratory insertion. For example, iodide inhibits CO migratory insertion in the Cativa process, and halide abstractors can be used to achieve high activity. In our prior work with pincer-crown ether ligands, we also observed CO insertion in cationic species $[\kappa^4-(^{15c5}NCOP)Ir(^{13}CH_3)(CO)]^+$ was ~ 11 -fold faster than in neutral iodide species $\kappa^3-(^{15c5}NCOP)Ir(^{13}CH_3)(CO)(I).^{23}$

To directly assess migratory insertion at a cationic species, we generated a cationic dicarbonyl complex and examined acetyl formation reactivity. The cationic bis(carbonyl) species with BAr^F₄⁻

anion (Ar^F = 3,5-bis(trifluoromethyl)phenyl), [(MeO-EtNCOP)Ir(CH₃)(CO)₂][BAr^F₄] ([7][BAr^F₄]), was synthesized from the reaction of **4-cis** with NaBAr^F₄ under a CO atmosphere (Scheme 4). CD₂Cl₂ solutions of [7][BAr^F₄] display a methyl resonance at δ –8.57 (d, J_{PC} = 6.8 Hz) in ¹H NMR spectra and two carbonyl resonances at δ 171.54 (s) and 167.41 (d, J_{PC} = 5.4 Hz) in ¹³C NMR spectra. The CO stretching frequencies of [7][BAr^F₄] observed by IR spectroscopy (ν_{co} = 2105, 2064 cm⁻¹) are higher energy than those of **4-cis** (2023 cm⁻¹) and **5-cis** (2015 cm⁻¹), confirming that the carbonyl ligands are more electrophilic in [7]⁺.

Scheme 4. Generation of acetyl via cationic species formation.

$$\begin{array}{c} \text{MeO} \\ \text{O} \\ -\text{P}^{\text{i}}}\text{P}^{\text{i}}\text{P}^{\text{i}}\text{P}^{\text{i}}\text{P}^{\text{i}}\text{P}^{\text{i}}}\text{P}^{\text{i}}\text{P}^{\text{i}}\text{P}^{\text{i}}\text{P}^{\text{i}}}\text{P}^{\text{i}}\text{P}^{\text{i}}\text{P}^{\text{i}}\text{P}^{\text{i}}\text{P}^{\text{i}}}\text{P}^{\text{i}}\text{P}^{\text{i}}\text{P}^{\text{i}}\text{P}^{\text{i}}\text{P}^{\text{i}}\text{P}^{\text{i}}\text{P}^{\text{i}}}\text{P}^{\text{i}}\text{P}^{\text{i}}\text{P}^{\text{i}}\text{P}^{\text{i}}\text{P}^{\text{i}}\text{P}^{\text{i}}\text{P}^{\text{i}}\text{P}^{\text{i}}\text{P}^{\text{i}}\text{P}^{\text{i}}}\text{P}^{\text{i}}\text{P}^{\text{i}}\text{P}^{\text{i}}\text{P$$

The cationic species [7][BAr^F₄] underwent CO insertion in acetonitrile, as predicted.²³ Thermolysis of [7][BAr^F₄] in CD₃CN at 80 °C under 1 atm CO for 10 h resulted in ~60% yield of a new species (31 P{ 1 H} NMR δ 141.61) with a diagnostic acetyl peak (1 H NMR δ 1.82, s) indicative of [($^{MeO-Et}$ NCOP)Ir(COCH₃)(CO)₂][BAr^F₄] ([8][BAr^F₄]). Unfortunately, we were unable to isolate [8][BAr^F₄] because removal of the CO atmosphere resulted in reversion to [7][BAr^F₄] (Scheme 4).

The combined results are consistent with acetyl formation requiring acetate dissociation to reach a cationic intermediate capable of CO migratory insertion. Accordingly, only 25% conversion of

[7][BAr^F₄] to [8][BAr^F₄] was observed in the presence of (mostly insoluble) LiOAc in CD₃CN under 1 atm CO over 50 h at 80 °C. Complete inhibition of migratory insertion is observed in the presence of tetrabutylammonium acetate, with immediate formation of **4-cis** and **4-trans** and no detectable [8][BAr^F₄]. Whereas these data show that acetate binds strongly to iridium in acetonitrile (acetate dissociation is unfavorable), acetate dissociation to produce cationic iridium species is much more facile in methanol. In fact, [7][OAc] formed *in situ* in methanol under CO has almost identical spectral features to [7][BAr^F₄] in methanol. Formation of the cationic dicarbonyl complex enables rapid migratory insertion.

Comparing acetate and iodide ligands in CO insertion and methyl acetate formation. Little is known about how migratory insertion and organic acetyl liberation will change based on the presence of iodide or acetate ligands, but differences in reactivity in these later steps of the proposed catalytic cycle could be important in iodide-free carbonylation processes. In fact, there is relatively little mechanistic information of any kind on reductive elimination processes relevant to methanol carbonylation, 3,25–27 and some reports point to methanolysis while others propose C–I reductive elimination to produce acetyl iodide as an intermediate. 3,25–27,36,37

The reactivity of iodide species **5-cis** was examined under CO in order to compare with the previously described reactivity of acetate complex **4-cis**. Due to poor solubility of **5-cis** in CD₃OD, **5-cis** was dissolved in a mixture of 90% CD₃OD and 10% 1,2-dichloroethane (DCE) and charged with 1 atm CO. At ambient temperature, relatively little iodide dissociation was observed. After 24 h the mixture comprised unreacted **5-cis**, the isomer where the CO is *trans* to methyl (MeO-EtNCOP)Ir(CH₃)(I)(CO) (**5-trans**), and ~40% yield of [**7**]⁺. This contrasts the behavior of **4-cis**, which generated 70% yield of [**7**]⁺ after only 5 h (*vide supra*), indicating that iodide dissociation is less favorable than acetate dissociation in MeOH solvent. Heating this mixture for 3 h at 65 °C

led to ~40% conversion to two iridium carbonyl products, **6** and iridium(III) hydridoiodide species ($^{\text{MeO-Et}}$ NCOP)Ir(H)(CO)(I) (**10**), identified by a hydride resonance in the 1 H NMR spectrum (δ – 16.64, d, J_{PH} = 19.4 Hz), in ~1:8 ratio. The formation of hydridoiodide **9** is similar to our previous study of a crown-ether-containing iodide complex, 22 but contrasts the reactivity of **4-cis** to produce only iridium(I) carbonyl **6**. This raises the possibility that one role of iodide is to shift speciation away from iridium(I) carbonyl, which could have important implications in catalysis. For example, hydride complexes are proposed to be responsible for catalyzing the undesired water-gas shift reaction as a side-reaction during the Cativa process. 1,3,26,38

To better compare the influence of acetate and iodide ligands on acetyl formation, the kinetics of CO insertion of iodide (5-cis) and acetate (4-cis) complexes were studied. The kinetics were first compared in CD₃OD/DCE (8:2) solution, since 5-cis is insoluble in pure methanol (Table 1). Samples containing 16 mM Ir were prepared in the glovebox, charged with 1 atm CO, and heated at 65 °C. The reaction progress was followed by ¹H and ³¹P{¹H} NMR spectroscopy. Since the Ir iodide and acetate complexes establish an equilibrium mixture of cis/trans isomers and the dicarbonyl cation [7]⁺ under CO in MeOH, the total amount of methyl species was used to evaluate the half-life under pseudo-first order conditions (see the SI for details).

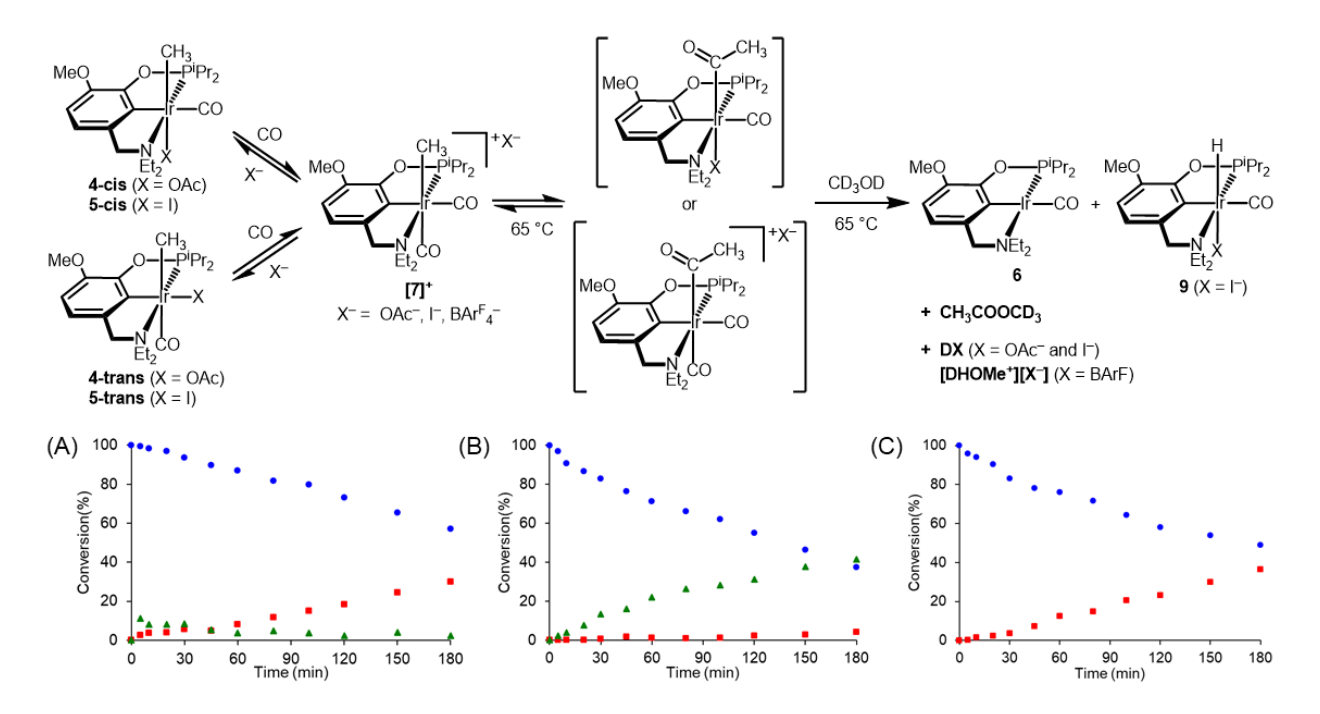


Figure 5. Kinetics of CO insertion and reductive elimination with (A) **5-cis**, (B) **4-cis** and (C) **[7][BAr^F₄]** in CD₃OD/DCE (8:2) solution. Consumption of sum of the methyl species (blue circle) and yields of the final carbonyl species (red square) and the acetyl intermediate (green triangle) are shown.

Table 1. Half-lives $(t_{1/2}, min)$ for conversion of **4-cis**, **5-cis** and [7][BAr^F₄] under 1 atm CO in methanol.^a

Solvent	Half-life for conversion (min)		
	5-cis ^b	4-cis ^b	[7][BAr ^F ₄]
CD ₃ OD/DCE (8:2)	250(10)	120(10)	140(30)
CD ₃ OD/DCE (9:1)	270°	72	120
CD ₃ OD only	_c	69	95

^aReactions were heated at 65 °C and monitored by ¹H and ³¹P{¹H} NMR (25 °C); based on standard deviation of two trials in CD₃OD/DCE (8:2), expected uncertainty for other conditions is $\pm 10\%$. Half-life (t_{1/2}) is the time to 50% conversion based on an exponential fit of the decaying

signal for the Ir methyl complex (first $\sim 35\%$ conversion; see the Experimental Section for details). ^bThe inverse-gated ³¹P{¹H} NMR integrals for each methyl species disappearing was summed to a single integral and plotted to obtain a weighted average half-life. ^c5-cis is insoluble in MeOH only.

The iodide species (a mixture of **5-cis**, **5-trans**, and **[7][I]**) were consumed with $t_{1/2} = 250$ min, as the two Ir carbonyl products **6** and **9** appeared (Figure 5a). Only a small amount of an Ir acetyl intermediate ($^{31}P\{^{1}H\}$ NMR δ 140.46) was present during the reaction. This suggests a two-step sequence in which the initial migratory insertion is the rate-determining step.

The acetate species (a mixture of **4-cis**, **4-trans** and **[7][OAc]**) were consumed at a significantly faster rate, $t_{1/2} = 120 \text{ min}$ (Figure 5b). The reaction forms large amounts of an Ir acetyl intermediate ($^{31}P\{^{1}H\}$ NMR δ 141.92, ^{1}H NMR δ 1.81), before giving way to the product **6**, acetic acid, and methyl acetate after prolonged heating (*vide supra*). Here, reductive elimination of methyl acetate is the rate-determining step, but the distinct rates of each step enable independent kinetic analysis of the initial migratory insertion step.

4-cis is consistent with the lesser degree of iodide dissociation relative to acetate dissociation observed for this complex, which limits access to the needed cationic intermediate [7]⁺ for CO insertion. The trend is opposite for the reductive elimination step, however, with the iodide complex supporting faster methyl acetate formation. The difference could be due to a lower barrier kinetic pathway to formation of acetyl iodide as an intermediate that reacts with methanol to produce methyl acetate, as is typically proposed in the Cativa process. ¹⁻⁵ The labeling study above (see Scheme 3) established that reactions starting from acetate complex 4-cis produce methyl acetate directly via coupling of methanol and the acetyl. Consistent with this hypothesis, ²⁵ the reaction of 4-cis proceeded faster as the methanol content was increased (Table 1), entering a

regime where the second step starts to influence the rate of methyliridium complex conversion, reaching a maximum in pure CD₃OD, $t_{1/2} = 69$ min. No such methanol promotion is observed for the iodide complex, which is more consistent with an iodide/acetyl reductive elimination pathway.

If the faster rate of migratory insertion of acetate complex **4-cis** is due to accessing a cationic dicarbonyl intermediate, the cationic species with a BAr^F₄ counter anion, [7][BAr^F₄], should exhibit similar kinetics. As shown in Figure 5c, [7][BAr^F₄] was consumed at almost the same rate as **4-cis**, consistent with our prediction (t_{1/2} of 140 min). This is consistent with migratory insertion from similar cationic species [7]⁺ in both cases. Surprisingly, however, no acetyl intermediate was observed and the reaction promptly generated Ir carbonyl product **6**. Methanol is again indicated to be the nucleophile, based on faster rates with higher methanol content (Table 1). The faster rate of reductive elimination in [7][BAr^F₄] may be rationalized by the lack of coordinating anion: DFT calculations suggest the acetyl intermediate derived from **4-cis** re-binds acetate, which would slow down reductive elimination relative to the cationic acetyl derived from [7][BAr^F₄] (Figure 6). Acetate binding *trans* to the acetyl ligand is ca. 8 kcal/mol more favorable than acetate binding *trans* to the methyl ligand (Table S12 and S14), suggesting that while acetate dissociation to form a cationic methyl complex is accessible, re-binding of acetate after migratory insertion may inhibit methyl acetate formation.

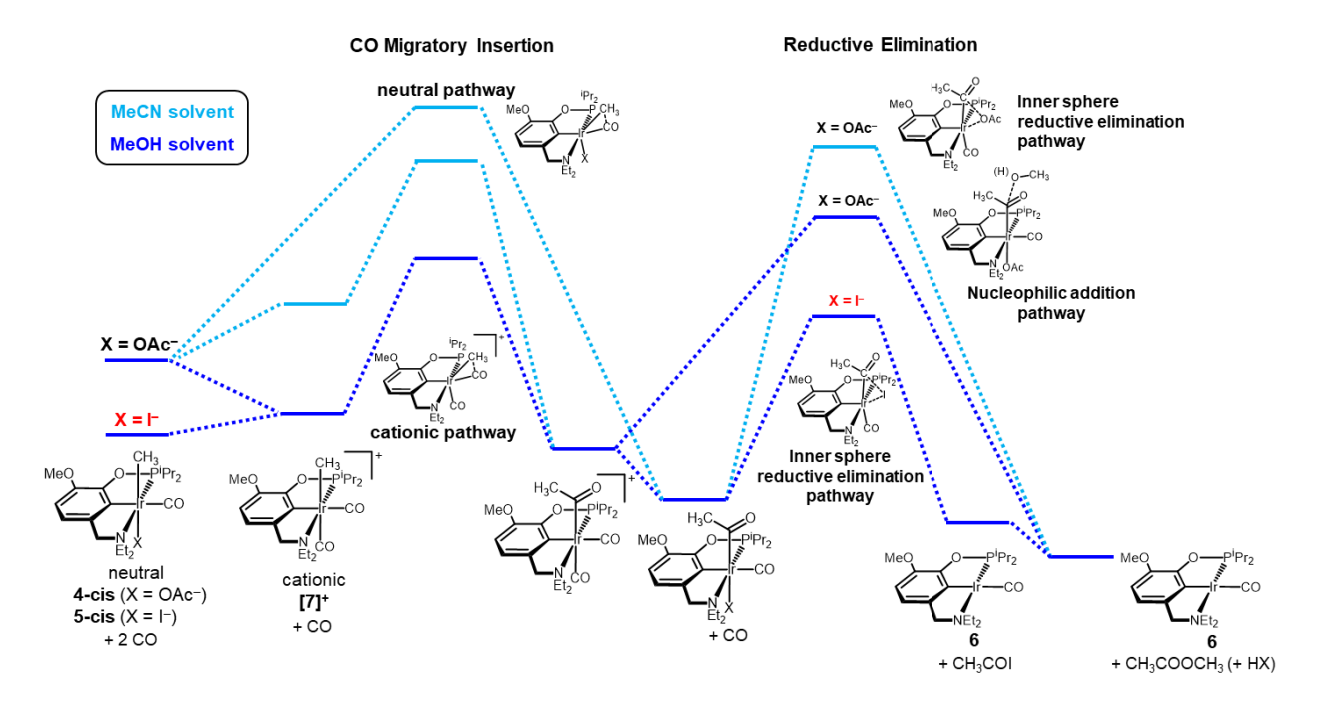


Figure 6. Free energy landscape of carbonylation of iridium methyl compounds comparing effect of anion and solvent.

Figure 6 summarizes the anion and solvent effects on CO migratory insertion and reductive elimination. Methanol solvation promotes acetate dissociation from **4-cis** to produce a cationic methyl species [7]⁺ that has a much lower activation barrier for CO migratory insertion than the neutral pathway. Iodide ions inhibit migratory insertion according to the same principles, due to preferential halide association to the iridium center that inhibits access to key intermediate [7]⁺. Methanol solvent is also essential for methyl acetate reductive elimination, via either a concerted inner sphere mechanism producing acetyl iodide that reacts with methanol or an outer sphere nucleophilic addition mechanism. The acetate complex is proposed to undergo outer sphere reductive elimination by methanol addition to a cationic acetyl intermediate, as indicated by labeling studies and the observation that methyl acetate is produced more rapidly with [7][BAr^F₄].

In the presence of iodide, methyl acetate formation is faster, which we attribute to accessing an inner sphere C–I reductive elimination mechanism.

Conclusions. An iodide-free carbonylation reaction sequence is reported, based on net C—O bond activation of methyl acetate by a pincer iridium(I) complex followed by CO insertion and formation of acetic acid and another equivalent of methyl acetate (Scheme 5). The net reaction is methanol carbonylation to acetic acid, with methyl acetate acting as a methylating promoter (and with additional conversion of an iridium(I) dinitrogen complex to an iridium(I) carbonyl complex).

Scheme 5. Summary of the carbonylation reaction via methyl acetate C–O activation.

The carbonylation sequence provides a unique opportunity to understand how iodide and acetate influence various individual steps relevant to carbonylation catalysis. The CO migratory insertion is strongly solvent dependent. In methanol, acetate complexes undergo fast migratory insertion, attributed to facile acetate substitution by CO to form a cationic dicarbonyl intermediate that facilitates CO insertion. In dichloromethane or acetonitrile, however, CO migratory insertion

was not observed, presumably due to unfavorable acetate substitution by CO. The acetate complex undergoes migratory insertion more than twice as fast as the iodide complex in methanol. The faster rate of C–C bond formation with an acetate ligand is attributed to more favorable formation of a cationic methyl dicarbonyl intermediate by acetate substitution relative to iodide substitution in methanol.

Experimental data on acetyl reductive elimination are particularly lacking for iridium-catalyzed carbonylation.^{3,25–27} Here, we find evidence for distinct reductive elimination pathways in the presence of acetate and iodide. In methanol solvent, iodide complexes undergo faster elimination than acetate complexes, and the rate does not increase with higher concentrations of methanol. This suggests a direct reductive elimination of acetyl iodide occurs first, followed by reaction with the solvent methanol to generate methyl acetate. In iodide-free conditions, the solvent methanol is the reductive elimination partner, directly generating methyl acetate in a reaction that is proceeds faster when the concentration of methanol increases.

The major current limitation is that the reaction is not catalytic, because (a) the resulting iridium(I) carbonyl complex does not readily react with MeOAc to re-form a methyliridium complex and (b) the solvents for methylation and acetylation are incompatible (Scheme 5). Further work is needed to find a system capable of facile activation of methyl acetate in the presence of CO, and reaction conditions that can support all the elementary steps of the carbonylation process. Our observations of individual steps in an iodide-free carbonylation scheme may aid in future development of iodide-free carbonylation catalysts, and provide rare insight into reductive elimination processes that furnish organic acetyls.

ASSOCIATED CONTENT

Supporting Information. The Supporting Information is available free of charge on the ACS Publications website.

Experimental details and characterization data (PDF)

DFT coordinates (XYZ)

Crystallographic data for 2 and 5-cis (CIF)

CCDC Deposition numbers 2084756-2084757

AUTHOR INFORMATION

Corresponding Author

* ajmm@email.unc.edu

ACKNOWLEDGMENT

Eastman Chemical Co. is gratefully acknowledged for financial support. The authors thank Faraj Hasanayn (American University Beirut) for assistance with computational studies and Josh Chen (UNC-CH) for assistance with X-ray crystallography. The NMR spectroscopy was supported by the National Science Foundation under Grant No. CHE-1828183 and Grant No. CHE-0922858. The mass spectrometry was supported by the National Science Foundation under Grant No. CHE-1726291.

REFERENCES

- (1) Le Berre, C.; Serp, P.; Kalck, P.; Torrence, G. P. Acetic Acid. In *Ullmann's Encyclopedia* of *Industrial Chemistry*; Wiley-VCH Verlag GmbH & Co. KGaA: Weinheim, Germany, 2014; Vol. 10, pp 1–34. https://doi.org/10.1002/14356007.a01 045.pub3.
- (2) Kalck, P.; Le Berre, C.; Serp, P. Recent Advances in the Methanol Carbonylation Reaction into Acetic Acid. *Coord. Chem. Rev.* 2020, 402, 213078. https://doi.org/10.1016/j.ccr.2019.213078.
- (3) Morris, G. Carbonylation of Methanol to Acetic Acid and Methyl Acetate to Acetic Anhydride. In *Mechanisms in Homogeneous Catalysis*; Wiley-VCH Verlag GmbH & Co. KGaA: Weinheim, FRG, 2005; Vol. 54, pp 195–230. https://doi.org/10.1002/3527605134.ch5.
- (4) Beller, M.; Steinhoff, B. A.; Zoeller, J. R.; Cole-Hamilton, D. J.; Drent, E.; Wu, X.; Neumann, H.; Ito, S.; Nozaki, K. Carbonylation. In *Applied Homogeneous Catalysis with Organometallic Compounds*; Wiley: Cambridge, 2017; pp 91–190. https://doi.org/10.1002/9783527651733.ch3.
- (5) Maitlis, P. M.; Haynes, A.; James, B. R.; Catellani, M.; Chiusoli, G. P. Iodide Effects in Transition Metal Catalyzed Reactions. *Dalt. Trans.* 2004, No. 21, 3409–3419. https://doi.org/10.1039/b410128f.
- (6) Haynes, A. Acetic Acid Synthesis by Catalytic Carbonylation of Methanol. In *Catalytic Carbonylation Reactions*; Springer Berlin Heidelberg, 2006; Vol. 18, pp 179–205. https://doi.org/10.1007/3418_021.

- Haynes, A.; Maitlis, P. M.; Morris, G. E.; Sunley, G. J.; Adams, H.; Badger, P. W.;
 Bowers, C. M.; Cook, D. B.; Elliott, P. I. P.; Ghaffar, T.; Green, H.; Griffin, T. R.; Payne,
 M.; Pearson, J. M.; Taylor, M. J.; Vickers, P. W.; Watt, R. J. Promotion of IridiumCatalyzed Methanol Carbonylation: Mechanistic Studies of the Cativa Process. *J. Am. Chem. Soc.* 2004, *126* (9), 2847–2861. https://doi.org/10.1021/ja039464y.
- (8) Bagno, A.; Bukala, J.; Olah, G. A. Chemistry in Superacids. 8. Superacid-Catalyzed Carbonylation of Methane, Methyl Halides, Methyl Alcohol, and Dimethyl Ether to Methyl Acetate and Acetic Acid. *J. Org. Chem.* 1990, 55 (14), 4284–4289. https://doi.org/10.1021/jo00301a015.
- (9) Wegman, R. W. Vapour Phase Carbonylation of Methanol or Dimethyl Ether with Metal-Ion Exchanged Heteropoly Acid Catalysts. *J. Chem. Soc. Chem. Commun.* 1994, 947. https://doi.org/10.1039/c39940000947.
- (10) Ellis, B.; Howard, M. J.; Joyner, R. W.; Reddy, K. N.; Padley, M. B.; Smith, W. J. Heterogeneous Catalysts for the Direct, Halide-Free Carbonylation of Methanol. In *Studies in Surface Science and Catalysis*; 1996; Vol. 101 B, pp 771–779. https://doi.org/10.1016/S0167-2991(96)80288-6.
- (11) Blasco, T.; Boronat, M.; Concepción, P.; Corma, A.; Law, D.; Vidal-Moya, J. A.
 Carbonylation of Methanol on Metal–Acid Zeolites: Evidence for a Mechanism Involving
 a Multisite Active Center. *Angew. Chem. Int. Ed.* 2007, 46 (21), 3938–3941.
 https://doi.org/10.1002/anie.200700029.

- (12) Boronat, M.; Martínez-Sánchez, C.; Law, D.; Corma, A. Enzyme-like Specificity in Zeolites: A Unique Site Position in Mordenite for Selective Carbonylation of Methanol and Dimethyl Ether with CO. *J. Am. Chem. Soc.* **2008**, *130* (48), 16316–16323. https://doi.org/10.1021/ja805607m.
- (13) Ni, Y.; Shi, L.; Liu, H.; Zhang, W.; Liu, Y.; Zhu, W.; Liu, Z. A Green Route for Methanol Carbonylation. *Catal. Sci. Technol.* **2017**, *7* (20), 4818–4822.
 https://doi.org/10.1039/c7cy01621b.
- (14) Meng, X.; Yuan, L.; Guo, H.; Hou, B.; Chen, C.; Sun, D.; Wang, J.; Li, D. Carbonylation of Methanol to Methyl Acetate over Cu/TiO₂-SiO₂ Catalysts: Influence of Copper Precursors. *Mol. Catal.* **2018**, *456*, 1–9. https://doi.org/10.1016/j.mcat.2018.06.022.
- (15) Qi, J.; Christopher, P. Atomically Dispersed Rh Active Sites on Oxide Supports with Controlled Acidity for Gas-Phase Halide-Free Methanol Carbonylation to Acetic Acid. *Ind. Eng. Chem. Res.* 2019, 58 (28), 12632–12641. https://doi.org/10.1021/acs.iecr.9b02289.
- (16) Tong, C.; Zhang, J.; Chen, W.; Liu, X.; Ye, L.; Yuan, Y. Combined Halide-Free Cu-Based Catalysts with Triple Functions for Heterogeneous Conversion of Methanol into Methyl Acetate. *Catal. Sci. Technol.* 2019, *9* (21), 6136–6144. https://doi.org/10.1039/C9CY01321K.
- (17) Zoeller, J. R.; Moore, M. K.; Vetter, A. J. CARBONYLATION PROCESS. US7582792, 2009.

- (18) Ittel, S. D.; Tolman, C. A.; English, A. D.; Jesson, J. P. The Chemistry of 2-Naphthyl Bis[Bis(Dimethylphosphino)Ethane] Hydride Complexes of Fe, Ru, and Os. 2. Cleavage of sp and sp³ C-H, C-O, and C-X Bonds. Coupling of Carbon Dioxide and Acetonitrile. *J. Am. Chem. Soc.* **1978**, *100* (24), 7577–7585. https://doi.org/10.1021/ja00492a024.
- (19) Trovitch, R. J.; Lobkovsky, E.; Bouwkamp, M. W.; Chirik, P. J. Carbon–Oxygen Bond Cleavage by Bis(Imino)Pyridine Iron Compounds: Catalyst Deactivation Pathways and Observation of Acyl C–O Bond Cleavage in Esters. *Organometallics* **2008**, *27* (23), 6264–6278. https://doi.org/10.1021/om8005596.
- (20) Manbeck, K. A.; Kundu, S.; Walsh, A. P.; Brennessel, W. W.; Jones, W. D. Carbon—Oxygen Bond Activation in Esters by Platinum(0): Cleavage of the Less Reactive Bond.

 *Organometallics 2012, 31 (14), 5018–5024. https://doi.org/10.1021/om300323d.
- (21) Kundu, S.; Choi, J.; Wang, D. Y.; Choliy, Y.; Emge, T. J.; Krogh-Jespersen, K.; Goldman, A. S. Cleavage of Ether, Ester, and Tosylate C(sp³)–O Bonds by an Iridium Complex, Initiated by Oxidative Addition of C–H Bonds. Experimental and Computational Studies. *J. Am. Chem. Soc.* 2013, *135* (13), 5127–5143. https://doi.org/10.1021/ja312464b.
- (22) Gregor, L. C.; Grajeda, J.; White, P. S.; Vetter, A. J.; Miller, A. J. M. M. Salt-Promoted Catalytic Methanol Carbonylation Using Iridium Pincer-Crown Ether Complexes. *Catal. Sci. Technol.* **2018**, *8* (12), 3133–3143. https://doi.org/10.1039/c8cy00328a.
- (23) Gregor, L. C.; Grajeda, J.; Kita, M. R.; White, P. S.; Vetter, A. J.; Miller, A. J. M. Modulating the Elementary Steps of Methanol Carbonylation by Bridging the Primary and

- Secondary Coordination Spheres. *Organometallics* **2016**, *35* (17), 3074–3086. https://doi.org/10.1021/acs.organomet.6b00607.
- (24) Yoo, C.; Dodge, H. M.; Farquhar, A. H.; Gardner, K. E.; Miller, A. J. M. Decarbonylative Ether Dissection by Iridium Pincer Complexes. *Chem. Sci.* **2020**, *11* (44), 12130–12138. https://doi.org/10.1039/d0sc03736b.
- (25) Matsumoto, T.; Mizoroki, T.; Ozaki, A. Mechanistic Study of Methanol Carbonylation Catalyzed by an Iridium Complex in the Presence of Methyl Iodide. *J. Catal.* **1978**, *51* (1), 96–100. https://doi.org/10.1016/0021-9517(78)90242-7.
- (26) Forster, D. Kinetic and Spectroscopic Studies of the Carbonylation of Methanol with an Iodide-Promoted Iridium Catalyst. *J. Chem. Soc. Dalt. Trans.* 1979, 1639–1645. https://doi.org/10.1039/DT9790001639.
- (27) Kinnunen, T.; Laasonen, K. Reaction Mechanism of the Reductive Elimination in the Catalytic Carbonylation of Methanol. A Density Functional Study. *J. Organomet. Chem.* 2001, 628 (2), 222–232. https://doi.org/10.1016/S0022-328X(01)00800-2.
- (28) Choi, J.; Choliy, Y.; Zhang, X.; Emge, T. J.; Krogh-Jespersen, K.; Goldman, A. S. Cleavage of sp³ C–O Bonds via Oxidative Addition of C–H Bonds. *J. Am. Chem. Soc.* **2009**, *131* (43), 15627–15629. https://doi.org/10.1021/ja906930u.
- (29) Haibach, M. C.; Lease, N.; Goldman, A. S. Catalytic Cleavage of Ether C-O Bonds by Pincer Iridium Complexes. *Angew. Chem. Int. Ed.* **2014**, *53* (38), 10160–10163. https://doi.org/10.1002/anie.201402576.

- (30) Chapp, S. M.; Schley, N. D. Evidence for Reversible Cyclometalation in Alkane Dehydrogenation and C–O Bond Cleavage at Iridium Bis(Phosphine) Complexes. *Organometallics* 2017, 36 (22), 4355–4358. https://doi.org/10.1021/acs.organomet.7b00676.
- (31) Rybtchinski, B.; Vigalok, A.; Ben-David, Y.; Milstein, D. A Room Temperature Direct Metal Insertion into a Nonstrained Carbon–Carbon Bond in Solution. C–C vs C–H Bond Activation. J. Am. Chem. Soc. 1996, 118 (49), 12406–12415. https://doi.org/10.1021/ja962253r.
- van der Boom, M. E.; Liou, S.; Ben-David, Y.; Gozin, M.; Milstein, D. Carbon–Carbon Bond Activation by Rhodium(I) in Solution. Comparison of sp²–sp³ vs sp³–sp³ C–C, C–H vs C–C, and Ar–CH₃ vs Ar–CH₂CH₃ Activation. *J. Am. Chem. Soc.* **1998**, *120* (51), 13415–13421. https://doi.org/10.1021/ja982345b.
- (33) Rybtchinski, B.; Milstein, D. Metal Insertion into C–C Bonds in Solution. *Angew. Chem. Int. Ed.* **1999**, *38* (7), 870–883. https://doi.org/10.1002/(SICI)1521-3773(19990401)38:7<870::AID-ANIE870>3.0.CO;2-3.
- (34) Pearson, J. M.; Haynes, A.; Morris, G. E.; Sunley, G. J.; Maitlis, P. M. Dramatic Acceleration of Migratory Insertion in [MeIr(CO)₂I₃]⁻ By Methanol and by Tin(II) Iodide. *J. Chem. Soc. Chem. Commun.* **1995**, 1045. https://doi.org/10.1039/c39950001045.
- (35) West, N. M.; Miller, A. J. M.; Labinger, J. A.; Bercaw, J. E. Homogeneous Syngas Conversion. *Coord. Chem. Rev.* **2011**, *255* (7–8), 881–898. https://doi.org/10.1016/j.ccr.2010.08.019.

- (36) Lassauque, N.; Davin, T.; Nguyen, D. H.; Adcock, R. J.; Coppel, Y.; Le Berre, C.; Serp, P.; Maron, L.; Kalck, P. Direct Involvement of the Acetato Ligand in the Reductive Elimination Step of Rhodium-Catalyzed Methanol Carbonylation. *Inorg. Chem.* 2012, *51* (1), 4–6. https://doi.org/10.1021/ic201574m.
- (37) Hanh Nguyen, D.; Lassauque, N.; Vendier, L.; Mallet-Ladeira, S.; Le Berre, C.; Serp, P.; Kalck, P. Reductive Elimination of Anhydrides from Anionic Iodo Acetyl Carboxylato Rhodium Complexes. *Eur. J. Inorg. Chem.* 2014, 2014 (2), 326–336. https://doi.org/10.1002/ejic.201300933.
- (38) Elliott, P. I. P.; Haak, S.; Meijer, A. J. H. M.; Sunley, G. J.; Haynes, A. Reactivity of Ir(III) Carbonyl Complexes with Water: Alternative by-Product Formation Pathways in Catalytic Methanol Carbonylation. *Dalt. Trans.* **2013**, *42* (47), 16538–16546. https://doi.org/10.1039/c3dt52092g.